Effective Controls of Fixed Capacitor-Thyristor Controlled Reactors for Power Quality Improvement in Shipboard Microgrids

Terriche, Yacine; Guerrero, Josep M.; Vasquez, Juan C.; Mutarraf, Muhammad Umair; Lashab, Abderezak; Mehrzadi, Mojtaba; Su, chun Lien

Published in:
I E E E Transactions on Industry Applications

DOI (link to publication from Publisher):
10.1109/TIA.2021.3058595

Publication date:
2021

Effective Controls of Fixed Capacitor-Thyristor Controlled Reactors for Power Quality Improvement in Shipboard Microgrids

Yacine Terriche, *Student Member, IEEE,* Chun-Lien Su, *Senior Member, IEEE,* Abderezak Lashab, *Member, IEEE,* Muhammad. U. Mutarraf, , *Student Member, IEEE,* Mojtaba Mehrzadi, Josep M. Guerrero, *Fellow, IEEE,* Juan C. Vasquez, *Senior Member, IEEE*

***Abstract*--Addressing power quality issues in shipboard micro-grids (SMs), which are mainly attributable to the increased installation of power converters, has received much attention recently. To this end, static var compensators (SVCs), such as thyristor switched capacitors (TSCs) and fixed capacitors-thyristor controlled reactors (FCs-TCRs), can be effective solutions. Controlling these compensators, however, is not a trivial task as it involves sophisticated operations, especially estimating the firing angle, which should be carried out based on some nonlinear equations. This paper aims to propose the application of some simple yet numerically efficient algorithms based on Bisection, Newton-Raphson, False Position, and Scant methods for estimating the firing angle of the FC-TCR. The effectiveness and robustness of these algorithms are demonstrated via modeling of the FC-TCR with the electrical power system of a practical hybrid ferry under MATLAB/Simulink environment, where the results proved that the enhanced power quality issues respect the IEC standards 61000-4-7/30. Furthermore, an experimental setup consists of a digital signal processor and a programmable source is used to demonstrate that these techniques can be effectively applied in real-time applications.**

***Index Terms*-- Fixed capacitors-thyristor controlled reactors, harmonics, power factor, firing angle estimation, power quality, shipboard micro-grids, static var compensators.**

I. Introduction

From the early of the last decades, the substitution of the mechanical power systems with electrical ones onboard shipboard microgrids (SMs) has been witnessing large attention [1], [2]. Indeed, this revolution provides several advantages such as better maneuverability, easier controllability, improved efficiency, and gaining larger space [3]. However, the implementation of the power electronic converters (PECs) causes considerable power quality issues such as harmonics contamination and voltage instability [1], [2]. The existence of harmonics onboard SMs does not only cause the malfunctioning of many devices, but it can as well threaten the lives of the crew/passengers [4]. Moreover, the large penetration of the power electronics devices affects the voltage stability in a phenomenon usually named as constant power load (CPL) [3]. Moreover, the circulation of the reactive power caused by the thrusters and other reactive loads affects the efficiency of the electrical power system and increases the losses [5]. According to the classifications standards and rules for ships that deal with power quality issues [6], the voltage and current distortion should be less than 5%, and in some cases, the voltages is allowed to be less than 8%, the power factor (PF) should be higher than 0.9, while the voltage sags and swells should not exceed 10% and 6%, respectively [1].

In order to cope with power quality issues, several solutions have been proposed in the literature. The installation of passive power filters (PPFs) was one of the traditional and most used techniques to reduce the harmonics, and compensate for a degree of the PF [7], [8]. Though this solution is cheap and easy to implement, it, however, struggles from several weaknesses such as fixed tuning, filtering selectivity, bulkiness, and the possibility of inducing the resonance. To overcome the weakness of the PPFs, the active power filters (APFs) have been proposed as an alternative [9], [10]. However, their application for SMs is limited due to several deficiencies such as high switching losses, high cost, inability to filter the high order harmonics, and the implementation and maintenance complexity. Besides, if the distortion of the voltage exceeds a certain limit (THD_V > 0.08-0.1) it results in shortening the lifetime of the DC link capacitor of the APFs [1], [11]. The Static Var Compensators (SVCs) can be an effective alternative to improve some of the power quality issues as they are a cost-effective solution, they have much lower switching losses, and can be applied in high power applications [12]. The fixed capacitor-thyristor controlled reactor (FC-TCR), which is one of the SVCs family can work as a PF compensator [13] or as a voltage balancer to ensure stability [14]. It can further

This work was supported by the VILLUM FONDEN under the VILLUM Investigator Grant 25920, Center for Research on Microgrids (CROM).

Y. Terriche, A. Lashab, M. Mutarraf, M. Mehrzadi, J. M. Guerrero, and J. C. Vasquez are with the Department of Energy Technology, Aalborg University, 9220 Aalborg, Denmark (e-mail: yte@et.aau.dk abl@et.aau.dk; mmu@et.aau.dk; meh@et.aau.dk; joz@et.aau.dk; Juq@et.aau.dk).

C. Su is with Department of Electrical Engineering National Kaohsiung University of Science and Technology Kaohsiung City 805, Taiwan (cls@nkust.edu.tw).

improve the harmonic distortion [11] where it has been demonstrated that in [15], [16] if the FC-TCR impedance is well designed it can perform as a low-pass filter. Hence, decreases both voltage and current harmonics beyond the cutoff frequency. Furthermore, the sophisticated technology of the FC-TCR that is based on the thyristors is much cheaper than the IGPTs of the APFs. Hence, this compensator is foreseen to be an efficient device for SMs.

One of the complicated challenges in controlling the FC-TCR is the estimation of the firing angle, which triggers the thyristors to adjust the supplied reactive power. The complexity of this step lies in the nonlinearity form of the mathematical equation that relates the firing angle to the desired variable inductance [17]. Therefore, in the recent literature, the authors sometimes mention the firing angle, but they do not show details on how it is linearized in a straightforward manner [18]–[23]. Most of the traditional solutions to solve this issue are attained by performing an offline calculation based on a lookup table, which is stored in the microprocessor [12], [13]. However, the lookup table can only offer approximate values under load variation. Moreover, the offline calculation cannot be adaptive under frequency drifts, which is a common issue in SMs. Furthermore, storing the data of the lookup table in the digital processor cards saturates their memory spaces, which consequently decreases their efficacy in performing multiple tasks. Though the application of numerical methods is very effective for solving the nonlinear equations [24], they did not, however, attract much attention for extracting the firing angle of the FC-TCR compensator. This paper is an extended version of [25], where four simple yet-effective numerical methods to estimate the firing angle of the FC-TCR compensator are proposed. These methods that are based on the Bisection (BS) method, Newton-Raphson (N-R) method, false position (FP), and Scant (SC) method have proved their efficacy in estimating the firing angle of the FC-TCR accurately even under load and frequency variation. Hence, enhances the FC-TCR performance and improves the efficiency of the electrical power system of the SM. In addition, more results that evaluate the dynamic behavior of the FC-TCR compensator under load variations are presented. Furthermore, the codes of the four above mentioned numerical methods that are written in C^{++} programming language and can be run in some softwares such as MATLAB are delivered in the Appendix. Based on thorough simulation analysis of a practical hybrid ferry that is performed under MATLAB/Simulink environment, it has been demonstrated that these techniques can effectively enhance the performance of the FC-TCR compensator, and therefore reduce the harmonics and improve the PF to meet the IEC standards 61000-4-7/30. Furthermore, the real time validation of these numerical methods have been conducted in an experimental setup that consists of a digital signal processor card based on dSPACE and programmable source to validate their low computation burden and ability to run in real-time Interface (R-T-I) platforms, where it has been demonstrated that the real time results match the simulation ones in estimating the firing angle.

The rest of the paper is organized as follows. In Section II, the challenge statement of modelling the FC-TCR with a focus on the firing angle is presented. Section III presents the proposed numerical methods that estimate the firing angle. Section IV presents simulation results and discussions. Section V addresses the real-time application of the proposed numerical methods and finally, Section VI concludes this paper.

II. Problem Statement

The basic circuit of the FC-TCR compensator contains a fixed capacitor connected in shunt with an inductance, where the value of the inductance can vary based on controlling two anti-parallel sophisticated valves that function alternatively each half-cycle [12]. These valves are controlled by estimating the firing angle that corresponds to the aimed injected reactive power. Fig. 1 (a) shows the electrical power system of the selected hybrid ferry in a single-line form. It comprises two parallel diesel generators that supply the power, two propellers, a bunch of batteries for energy storage, hotel loads, and the FC-TCR compensator. The number of running generators is decided by the power management system based on the load demand and fuel consumption efficiency. The energy storage system is installed to enhance the power supply, and thus reduces the fuel consumption and emissions. Fig. 1(b) presents a single line diagram of the FC- TCR connected to the electrical power system of the hybrid ferry, where R_{s1}, R_{s2}, X_{ls1}, X_{ls2} are respectively the resistances and reactances of the sub-transient reactance of the synchronous generators plus the line impedances. Z_{lo} is the load impedance. i_s, i_{Lo}, and i_{fi} are, respectively, the source, load, and filter currents. i_{hif}, i_{hil}, are the TCR and the load harmonic currents . i_{hi} is the summation of i_{hif} and i_{hil}. Fig. 1(c) is the harmonic circuit, which displays the movement of only the harmonics in the electrical power system and the FC-TCR compensator. The harmonic attenuation factor ∂, which exhibits the filtering capability of the FC-TCR is presented as

$$\partial = \frac{\left| \frac{(X_{LFi} + R_{LFi}) \cdot (X_{CFi} + R_{CFi})}{X_{LFi} + R_{LFi} + X_{CFi} + R_{CFi}} \right|}{\left| \frac{(X_{LFi} + R_{LFi}) \cdot (X_{CFi} + R_{CFi})}{X_{LFi} + R_{LFi} + X_{CFi} + R_{CFi}} + \frac{(X_{Ls1} + R_{Ls1}) \cdot (X_{Ls2} + R_{Ls2})}{X_{Ls1} + R_{Ls1} + X_{Ls2} + R_{Ls2}} \right|} \quad (1)$$

where X_{CFi} and X_{LFi} are the reactances of the capacitor and inductance of the FC-TCR compensator. If we neglect the resistors of the FC-TCR compensator and main impedance due to their low values compared to the inductances and we make some mathematical manipulations, (1) becomes:

$$\partial = \frac{1}{\left|1+\frac{(X_{LFi}+X_{CFi})}{(X_{LFi})\cdot(X_{CFi})}\frac{(X_{Ls1})\cdot(X_{Ls2})}{X_{Ls1}+X_{Ls2}}\right|} \quad (2)$$

Fig. 2 presents the harmonic attenuation factor in terms of the filter capacitance reactance and the line impedance which includes the sub-transient reactance of the synchronous generators. For the sake of simplicity we set $X_{ls} = (X_{Ls1})\cdot(X_{Ls2}) / X_{Ls1} + X_{Ls2}$. It is very obvious that either decreasing the FC-TCR capacitor or increasing X_{ls} value results in decreasing ∂, which consequently improves the filtering capability. The variation of X_{ls} occurs due to the redundancy of the synchronous generators by turning on/off the second generators to satisfy the load demand and enhances the fuel consumption efficiency.

The control of the FC-TCR can be achieved in two modes, one mode is for compensating the PF and the other mode is for ensuring voltage stability. In this paper, we will focus on the first mode to validate the efficacy of the proposed methods, though these methods can work effectively for the second mode as well. Fig. 3 depicts the control algorithm of the FC-TCR to compensate for the PF. The connection of the fixed capacitor overcompensate the reactive power by moving the PF from lagging PF into leading PF, then via the proposed control of the anti-parallel thyristors of the TCR, the PF is tended towards unity. The procedure starts by estimating the phases of the load voltage and load currents, respectively, using the discrete Fourier transform as

$$\phi_{V_{load}} = a\tan\left(\frac{\frac{1}{N}\sum_{K=0}^{N-1} V_{load}(K)(\cos(2\pi f K)}{\frac{1}{N}\sum_{K=0}^{N-1} V_{load}(K)(\sin(2\pi f K)}\right) \quad (3)$$

$$\phi_{I_{load}} = a\tan\left(\frac{\frac{1}{N}\sum_{K=0}^{N-1} I_{load}(K)(\cos(2\pi f K)}{\frac{1}{N}\sum_{K=0}^{N-1} I_{load}(K)(\sin(2\pi f K)}\right) \quad (4)$$

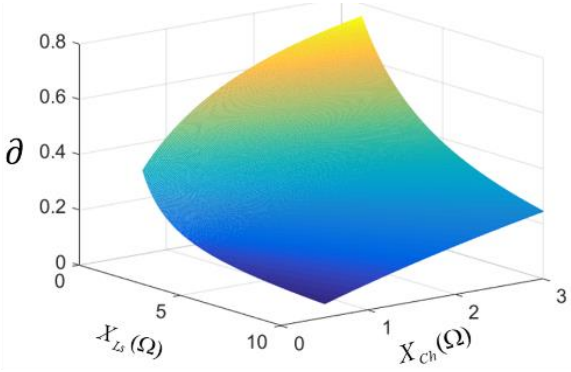

Fig. 2. Filtering capability of the FC-TCR compensator

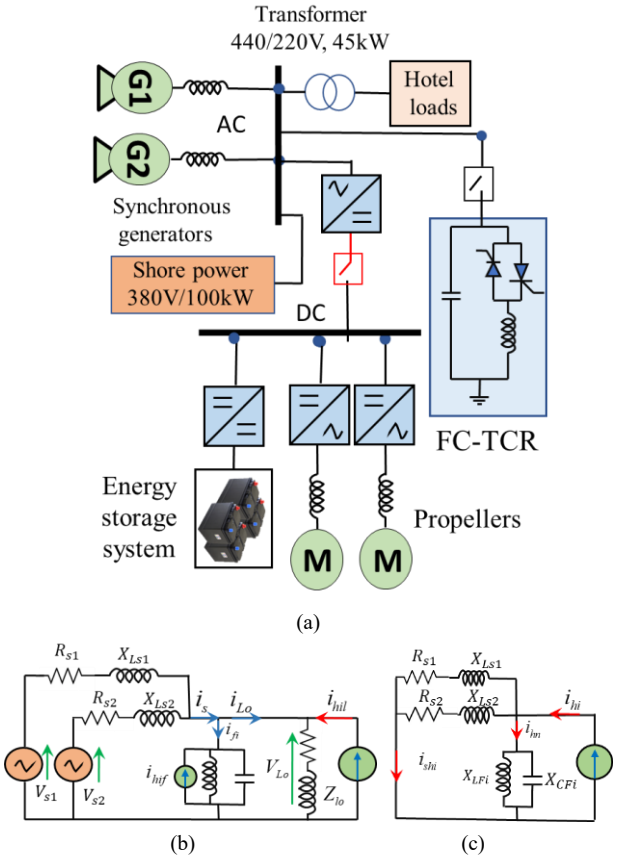

Fig. 1. Single line diagram of the FC-TCR compensator connected to the electrical power system of the hybrid ferry. (a) single line diagram of the electrical power system of the hybrid ferry. (b) per-phase base form circuit of (a). (c) equivalent harmonic circuit basic principle of Fig. (b) in a per-phase base form.

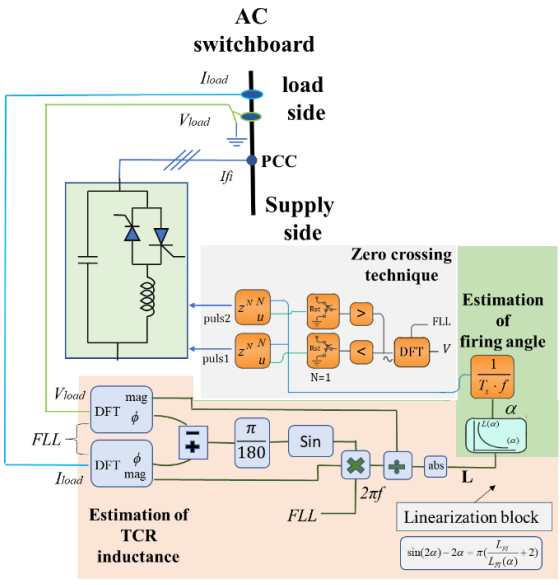

Fig. 3. Control algorithm of the FC-TCR to compensate for the power factor

$$mag_{V_{load}} = \sqrt{(\frac{1}{N}\sum_{K=0}^{N-1} V_{load}(K)(\sin(2\pi f\, K))^2 + (\frac{1}{N}\sum_{K=0}^{N-1} V_{load}(K)(\cos(2\pi f\, K))^2} \quad (5)$$

$$mag_{I_{load}} = \sqrt{(\frac{1}{N}\sum_{K=0}^{N-1} I_{load}(K)(\sin(2\pi f\, K))^2 + (\frac{1}{N}\sum_{K=0}^{N-1} I_{load}(K)(\cos(2\pi f\, K))^2} \quad (6)$$

where atan is the arctangent. N is the number of samples of one cycle. Then the magnitudes of the load voltage and load current are estimated as presented in equations (5) and (6) in the top of the next page. The reactive current, which circulates in the electrical power system is calculated as:

$$I_{reac} = mag_{I_{load}} \cdot \sin(\frac{\pi}{180}(\phi_{I_{load}} - \phi_{V_{load}})) \quad (7)$$

The calculation of the TCR inductance, which generates the appropriate amount of reactive power to tend the PF towards unity is calculated as

$$L_{Fi}(\alpha) = \frac{mag_{V_{load}}}{2 \cdot \pi \cdot f \cdot mag_{I_{load}}} \quad (8)$$

where $L_{Fi}(\alpha)$ is the inductance, which is obtained by controlling the firing angle α and indicates the amount of reactive power that is delivered by the TCR to tend the PF factor towards unity. The estimation of α is extracted from the following formula

$$\sin(2\alpha) - 2\alpha = \pi(\frac{L_{FI}}{L_{FI}(\alpha)} + 2) \quad (9)$$

where L_{Fi} is the inductance value of the TCR side. It is obvious that (9) is a non-linear equation, hence, the estimation of α is not straightforward. Traditional techniques to solve this issue apply offline calculations by estimating several values of α with different values of $L_{Fi}(\alpha)$ and then store the results in a lookup table in the microprocessor of the digital signal processor cards or computers [12], [13]. The first disadvantage of this method is the large space that data occupies in the memory of these cards that decreases their efficacy to perform multiples tasks. Moreover, as the offline calculation assumes the voltage magnitude and the frequency in (8) to be nominal, then under frequency drifts or voltages sags and swells, the accuracy of this method tends to worsen. In order to visualize this issue, uncertainties for voltage magnitudes and frequency are added to (8) to examine the system behavior as

$$L_{Fi}(\alpha) = \frac{mag_{V_{load}} \pm \Delta mag_{V_{load}}}{2 \cdot \pi \cdot (f \pm \Delta f) \cdot mag_{I_{load}}} \quad (10)$$

where $\Delta mag_{V_{load}}$ is the voltage sag or swell uncertainty, and Δf is the frequency uncertainty.

Substituting (10) in (9) results in

$$\sin(2\alpha) - 2\alpha = \pi(\frac{L_{FI}}{L_{FI}(\alpha) \cdot \Delta L_{FI}(\alpha)} + 2) \quad (11)$$

where $\Delta L_{FI}(\alpha)$ is the uncertainty caused by $\Delta mag_{V_{load}}$ and Δf .

Fig. 4 is portrayed to show the influence of $\Delta L_{FI}(\alpha)$ on the accuracy of α, where this latter varies from 90° to less than 180° that are the limits of the FC-TCR for a start connection.

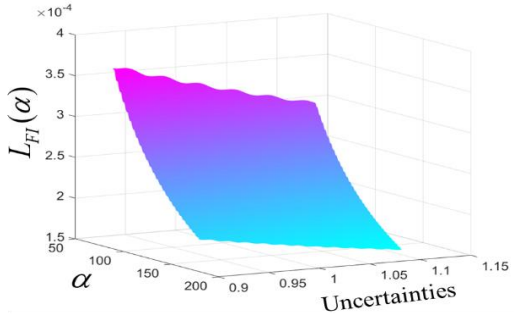

Fig. 4. Linearization of α under-voltage and frequency uncertainties

It is obvious that the variation of $\Delta L_{FI}(\alpha)$ affects the accuracy of α. However, when $\Delta L_{FI}(\alpha)$ is equal to unity, it implies that $\Delta mag_{V_{load}}$ and Δf have neglected values, which is barely impossible in SMs due to the pulsed heavy loads that absorb a large power in a short time. Thus, perturbs the voltage magnitude and frequency. In order to overcome the deficiencies of the lookup table, this paper examines the performance of four numerical methods in the next section that can estimate α accurately online without any stored data and can be adapted under variable grid conditions. After the estimation of α, the zero-crossing method is applied to extract the pulses of controlling the TCR.

III. Estimation of Firing Angles in FC-TCRs

The proposed methods are distinguished by the simplicity, low computation burden as their iterations are very few, they do not require any offline pre-calculation and they can be adapted under variable grid conditions. The main reason behind comparing these four methods is to assess their performance in terms of stabilization and the number of iterations in the case of controlling the FC-TCR compensator as they have different convergence behavior. For example, The NR method has a quadratic rate of convergence with only one initial guess, which means that if the function becomes flat at certain conditions the divergence will not be guaranteed. The BS method has, on the other hand, a linear convergence with two initial guesses set at a certain selected interval. Therefore, its convergence usually is slower than the NR, but it is guaranteed. The SC method has a superlinear convergence, but not very quadratic as the derivative applied in NR method is replaced by an approximation. Hence, this characteristic holds only for ordinary roots, and its convergence behavior changes in case the multiplicity of these roots are complex. Therefore, it is usually referred to as the quasi-Newton method. The FP method has a similar convergence linearity o the BS method. It is different from it only in the calculation for subdividing the interval of each

iteration. Hence, in some cases, it can be either faster or slower than the BS method.

A. Bisection Method

The bisection method is one of the simplest methods in numerical analysis, which is based on Bolzano's theorem to solve the transcendental equations by extracting the roots [24]. The main idea behind this approach is the intermediate hypothesis for continuous functions. It operates by tapering the gap located between the positive and negative intervals to the values that reach the correct answer with an accepted error. Fig. 5 depicts the flowchart of the BS method, which starts by identifying the variables of the non-linear function. In the studied case, the variable is the FC-TCR inductance $L_{Fi}(\alpha)$. The next step is to propose two initial guesses α_0 and β_0 for which $f(\alpha_0) > 0$ and $f(\beta_0) < 0$. The more α_0 and β_0 are close to the firing angle the fewer iterations the algorithm makes. As long as the firing angle of the FC-TCR is confined between $\pi/2 < \alpha < \pi$ in case of a star connection, it is easy to ensure a faster conversion of the method by setting the initial guests to $\alpha_0 = \pi/2$, $\beta_0 = \pi$ or nearby points. In order to provide further optimization to the algorithm, the guesses can be selected respectively to α that corresponds to the maximum and minimum reactive power of the system, respectively. Besides, an error should be selected that the system can tolerate. This error should provide a good compromise between the accuracy of the FC-TCR in compensating the reactive power and the computation burden of the algorithm, wherein it has been demonstrated in this paper that selecting the Error to 0.0001 provides a satisfactory accuracy with a very small number of iterations. After that, we define the non-linear equation of the FC-TCR, which is presented in (9). Once all these initial parameters are defined, the BS method starts calculating the arithmetic mean between α_0 and β_0 by narrowing the gap between the positive and negative intervals to estimate a midpoint until it reaches to the best approximation of the root as:

$$x_{i+1} = \frac{\alpha_i + \beta_i}{2} \tag{12}$$

where i starts from 0. Then the decision is made when $if\,(|x_{i+1}|) < error$, hence, outputs the desired value α as $\alpha = x_{i+1}$.

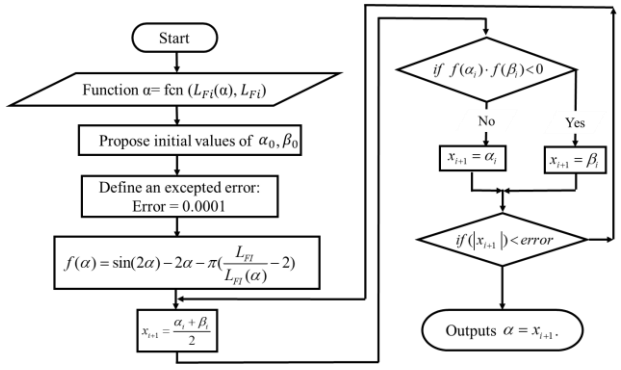

Fig. 5. The computational procedure of the Bisection method.

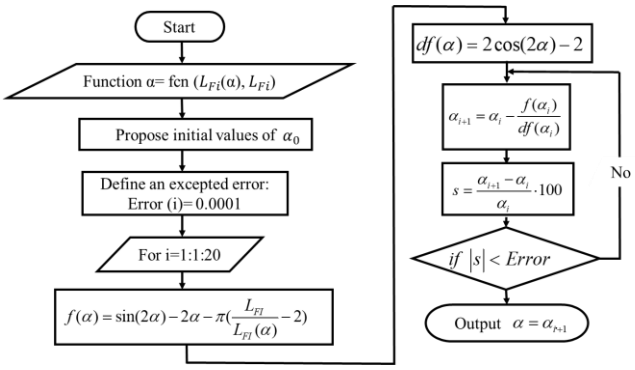

Fig. 6. The computational procedure of the Newton–Raphson method.

B. Newton–Raphson Method

In numerical analysis, the N–R method is one of the most applied techniques for root-finding that offers consecutively better approximations to the roots of a real-valued function [24]. Fig. 6 presents the N–R method flowchart, which starts by defining the value of L_{Fi} that is fixed, and the value of $L_{Fi}(\alpha)$ that is variable according to the reactive load variation.

The second step is to define an initial guess α_0. In contradiction with the BS method, the N–R method applies only one initial guess. As long as the firing angle of the FC-TCR is confined between $\frac{\pi}{2} < \alpha_0 < \pi$ in case of a star connection, then selecting α_0 within this range provides a faster convergence. The third step is to define an error, where the value of this error should not be high to ensure the accuracy of the FC-TCR, and should not be very small to decrease the number of iterations. Similar to the BS method, it will be demonstrated that setting Error= 0.0001 provides a good compromise between the accuracy and the number of iterations. After that, the N–R method linearization commence by defining the non-linear equation that is presented in (9) and its derivative that enables the calculation of α_{i+1}, which is expressed as:

$$\alpha_{i+1} = \alpha_i - \frac{f(\alpha_i)}{df(\alpha_i)} \tag{13}$$

After each iteration, the condition *S* is estimated as:

$$s = \frac{\alpha_{i+1} - \alpha_i}{\alpha_i} \cdot 100 \tag{14}$$

If *S* is less than the error, it implies that the algorithm reached a satisfactory true root and stops the calculation.

C. False Position Method

The FP method or regular false method is a root-finding algorithm in the numerical analysis [26]. This method depicted in Fig. 7 is similar to the BS method, where the difference between them lies in the improved adaptability of the FP method to larger dimensions such as systems of two or more non-linear equations. In order to motivate the FP method, two guesses values α_0 and β_0 needed to be defined for which

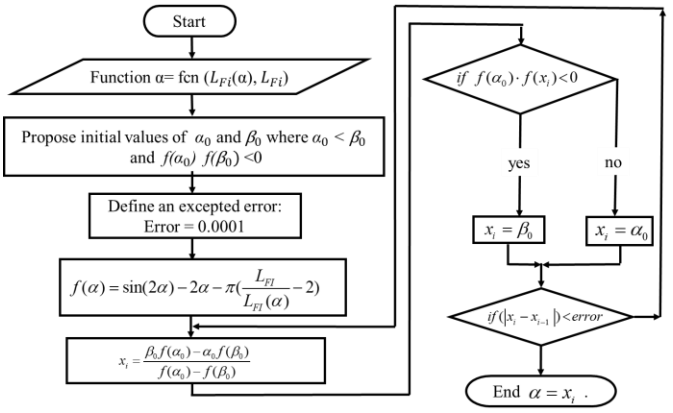

Fig. 7. The computational procedure of the False position method

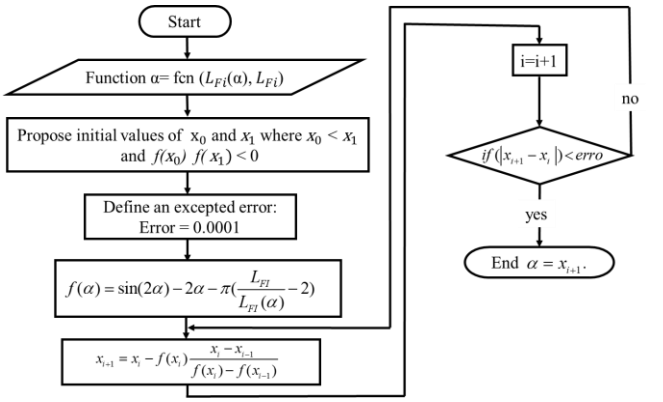

Fig. 8. The computational procedure of the Scant method

$f(\alpha_0) > 0$ and $f(\beta_0) < 0$. Similar to N–R and BS methods, an error should be defined, where the value of this error must provide a good compromise between the accuracy and computation burden. In this paper, the error for the FP method is selected to 0.0001 as it will be demonstrated in the results sections that this value provides efficient computation with a very accurate estimation of α. After that, the non-linear equation of the FC-TCR (see equation (9)), which provides the variable TCR inductance in function of α is defined. Once all these initial parameters are selected, the FP method commences by estimating the roots as

$$x_i = \frac{\beta_0 f(\alpha_0) - \alpha_0 f(\beta_0)}{f(\alpha_0) - f(\beta_0)} \tag{15}$$

The approximation of the roots during the iterations is obtained via selecting x_i either to be α_0 or β_0 depending on if the multiplication $if\ f(\alpha_0) \cdot f(x_i)$ is negative or positive. Once the approximation is less than the error ($(|x_i - x_{i-1}|) < error$), α is obtained with the last approximated roots.

D. Scant Method

The SC method is a root-finding algorithm in the numerical analysis to effectively approximate the roots of any given function $f(\alpha)$ with the lowest tolerated error [27]. This method is very similar to the false position method as both of them need to start the execution with two initial guesses to calculate the slope of the given function, which is utilized to project the x-axis for each new approximated root. The difference between them lies in the way of replacing the initial values with each new calculated root. For example, the FP method replaces each new calculated root with any of the original values producing a function value that contain a similar sign of $f(\alpha)$. As a result, the two estimates each time bracket the root, which enhances the convergence of the method. The secant method, on the other hand, replaces the approximated roots in strict order, where each new estimated root x_{i+1} that replaces x_i, and x_i that replaces x_1. This property can enable it to reach to the roots faster than the FP method in most cases. However, as the calculated values in some critical cases can lie on the same side of the new estimated root, it can lead to divergence in the worst cases if the initial guests are not well selected. Fig. 8 presents the flowchart of the SC method, which begins by defining L_{Fi}, $L_{Fi}(\alpha)$ and two guesses values x_0 and x_1, where $f(x_0) \cdot f(x_1) < 0$. Similar to the previous methods, an error should be defined, this error should be selected with a value that provides a good compromise between the accuracy and the number of iterations. In this paper, it will be validated that selecting the error to 0.0001 provides a very accurate estimation of α. Then, the equation of the FC-TCR that is presented in (9), which gives the variable TCR inductance in the function of α is inserted. Once all these initial parameters are selected, the SC method commences by estimating the roots as

$$x_{i+1} = x_i - f(x_i)\frac{x_i - x_{i-1}}{f(x_i) - f(x_{i-1})} \tag{16}$$

Once the approximation $|x_{i+1} - x_i|$ reaches to the first value that is less than the error, the algorithm breaks the calculation and outputs $x_{i+1} = \alpha$.

IV. Numerical Results and Discussions

The simulation results of a modelled practical hybrid electric ferry called Ferry Happiness are carried out under the MATLAB/Simulink environment. This Ferry is recently launched as a passenger ferry at Cijin Island in Kaohsiung city, Taiwan. Fig. 9 depicts the picture of the ferry and its electrical power system. The main system parameters are listed in Table I.

Fig. 10 presents the performance of the FC-TCR in harmonic filtering and PF compensation using the proposed numerical methods. The subplots of Fig. 10 present respectively the load voltage V_{Lo}, the load current i_{lo}, the source current i_s, the PF, the firing angle α, the number of iterations of each numerical method, the current of the TCR

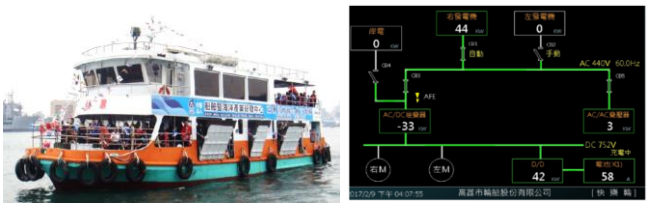

Fig. 9. Photo of the studied hybrid ferry and its electrical power system

TABLE I
SYSTEM PARAMETERS

Category	Parameters	Values
Synchronous generators	RMS voltage	V=450 V
	Electric Power	P= 2x88 ekW
propellers	Rated power	2x112 kW/1620 rpm
Hotel loads	Nominal power	P=35 ekW
PPFs	5th harmonic filter	$L = 0.006 / 0.016\ H$
		$C = 67.54/25.3302\ \mu F$
	7th harmonic filter	$L = 0.006 / 0.016\ H$
	Supporter inductance	$C = 34.46/12.92\ \mu F$
		$L_{sup} = 0.06\ H\ \ R = 2\Omega$

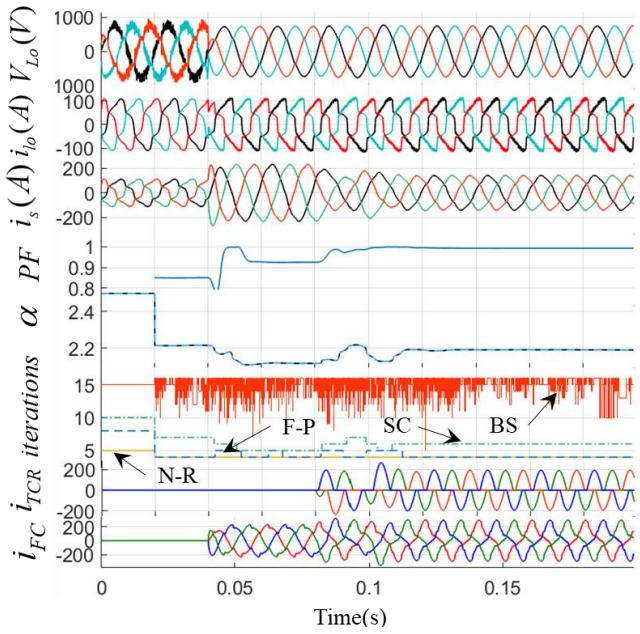

Fig. 10. Performance of the FC-TCR compensator based on the proposed numerical methods.

i_{TCR} , and the current of the fixed capacitor i_{FC} . It is clear that before connecting the FC-TCR, V_{Lo} and i_s are harmonically contaminated with a total harmonic distortion (THD) of about 19% and 15%, respectively.When connecting the switching capacitor in the instant 0.06s, it acts as a low-pass filter that filters all the harmonics after the cut-off frequency, hence, decreases the THDs of V_{lo} and i_s to less than 5%. Moreover, the connection of the switched capacitors drives the PF from lagging PF (0.89) to leading PF (0.94). Then, in the period 0.08s, the TCR is connected, where it is obvious that all the proposed numerical methods (N–R, BS, FP, SC) can accurately estimate α , hence, using the four methods gives the exact results. Besides, when connecting the FC-TCR in the instant 0.08s tends the PF from 0.94 to be close to unity. The last subplot displays the number of iterations of each numerical method. It is evident that, the N–R provides fewer iterations (from 4 to 6 iterations) compared to BS, FP, and SC methods during the variation of $L_{Fi}(\alpha)$. Moreover, the N–R is more simple and needs only one initial guess, which is usually selected in the middle of the interval $\frac{\pi}{2} < \alpha_0 < \pi$ (α_0 =135°), while the other methods need two initial guesses that lead to increase the iterations if they are not appropriately selected.

Fig. 11 presents the performance of the FC-TCR based on the proposed N–R method and the traditional lookup table for extracting the firing angle. Only the N–R method is selected in this study case since it provides the same accuracy as the other analyzed numerical methods with the smallest number of iterations. The subplots of Fig. 11 present respectively the RMS value of V_{Lo}, the RMS value of i_s , the firing angle, and the PF. It is clear that when connecting the switching capacitor in the period 0.03s, the PF moves from lagging PF to leading PF, then in the period 0.08s, the connection of the FC-TCR tends the PF closer to the unity. Though the lookup table method can extract the firing angle, it, however, struggles from some fluctuations, which consequently affects i_s that transmits them to V_{Lo} via the line impedance and the sub-transient reactance of the generators. However, estimating the firing angle using N–R method results in an accurate value of the PF without any fluctuations. Consequently, compensating the reactive current of i_s is accurate and free from fluctuations, which leads to a stable load voltage without any fluctuations.

Fig. 12 depicts the performance of the FC-TCR compensator under frequency drifts using the N–R method and the traditional lookup table. The subplots of Fig. 10 display respectively V_{Lo}, i_s , the RMS value of i_s , the firing angle, and the PF. It is evident that when connecting the switching capacitor in the period 0.03s, it results in filtering all the harmonics after the cut-off frequency, hence, decreases the THDs of V_{Lo} and i_s to less than 5%. Moreover, the reactive power generated by the switched capacitors moves the PF from lagging PF to leading PF. Then, in the period 0.06s, the connection of the FC-TCR compensates the PF to be close to unity. After that, in the period 0.12s, a frequency drift from 50 Hz to 52 Hz is caused to analyze the behavior of the FC-TCR compensator. It is obvious that the proposed method is flexible

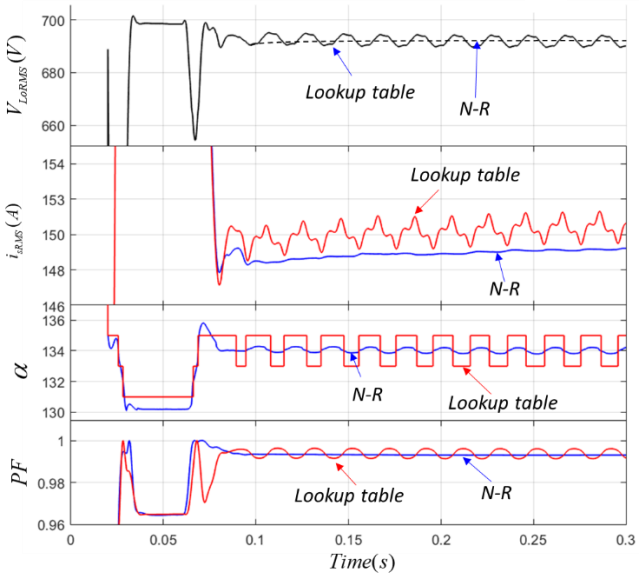

Fig. 11. Performance of the FC-TCR using the lookup table and N-R method.

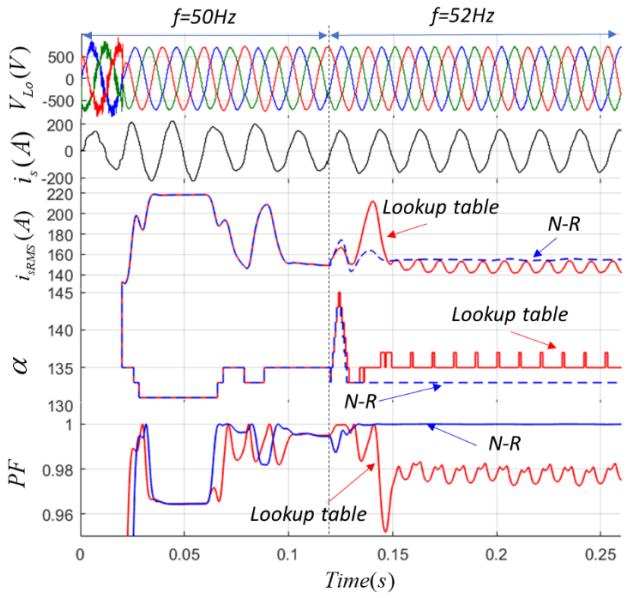

Fig. 12. Performance of the FC-TCR using the lookup table and N-R method under frequency drift.

during the variation of the frequency in estimating the firing angle accurately, which results in an accurate PF. Moreover, both PF and i_s that are estimated by the proposed method are free of fluctuations. On the other hand, the PF estimated by the traditional lookup table method is inaccurate due to the fact that the offline calculation is made based on assuming that the frequency of the system is nominal. Moreover, the firing angle estimated by the traditional lookup table struggles from some fluctuations that are well visualized on the PF subplot. These fluctuations result in effecting i_s as shown in the third subplot and can lead to voltage instability.

Fig. 13 presents the dynamic behavior of the FC-TCR compensator under load variation using the N–R method. The subplots of this figure present respectively the load voltage V_{Lo}, the compensated source current i_s, the distorted load current i_{lo}, the PF, the current of the TCR i_{TCR}, the current of the fixed capacitor i_{FC}, and the firing angle α. Before connecting the FC-TCR, it is obvious that both V_{lo} and i_s are harmonically distorted with THDs of respectively 19% and 15%. In the period 0.04s, the fixed capacitor is connected. As long as this capacitor is designed to act as a low-pass filter by decreasing the harmonic attenuation factor as presented in Fig. 2 it results in improving both V_{Lo} and i_s by decreasing the harmonics their THDs to less than 5%, which respects the IEC standards 61000-4-7/30. This evidence can be visualized in the waveform of i_{FC} that is harmonically contaminated due to the fact that the fixed capacitor absorbs the harmonics of the system. Moreover, the fixed capacitor pushes the lagging PF into leading PF. Then in the period 0.1s, the TCR is connected. It is evident that based on the accurate estimation of α using the N–R method, the TCR can accurately compensate for the PF to be close to unity. Furthermore, in the period 0.2s a load variation occurs. It is obvious that the FC-TCR compensator based on the proposed method can follow

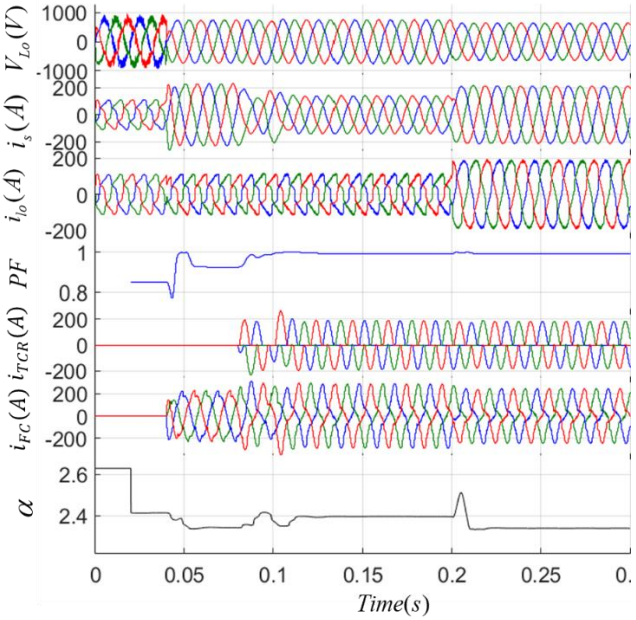

Fig. 13. Dynamic behavior of the FC-TCR using the N-R method under load variations

the load variation with a fast transient response (less than a cycle).

V. Experimental Results and Discussions

Fig. 14 presents the experimental bunch that is used to validate the capability of the applied numerical methods to work in real-time applications. The right side of Fig. 14 is a programmable source (model 61845), and the left side is the digital signal processor (dSPACE-1006). Though the FC-TCR is not available in the lab, the purpose of this verification is to ensure that these proposed numerical methods do not consume high computation burden and can effectively estimate the firing angle in real-time digital signal processor cards, which is the contribution of this paper. And validate that the real-time results match accurately the simulation results during the estimation of the firing angle.

Fig. 15 presents the real-time verification of the proposed numerical methods in estimating α. Fig. 15 (a) depicts the results obtained in the digital signal processor (dSPACE-1006) and Fig. 15 (b) presents the results obtained in Simulink. The subplots of Fig. 15 (a) and (b) present, respectively, the

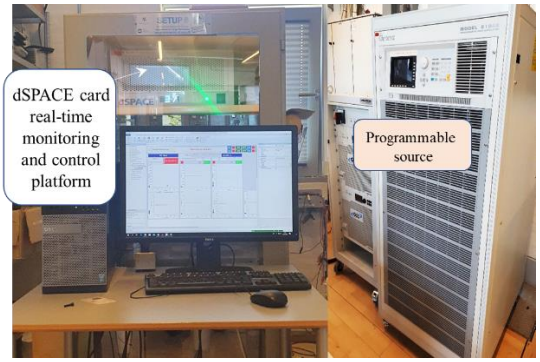

Fig. 14. Experimental setup for control and validation of the proposed approach.

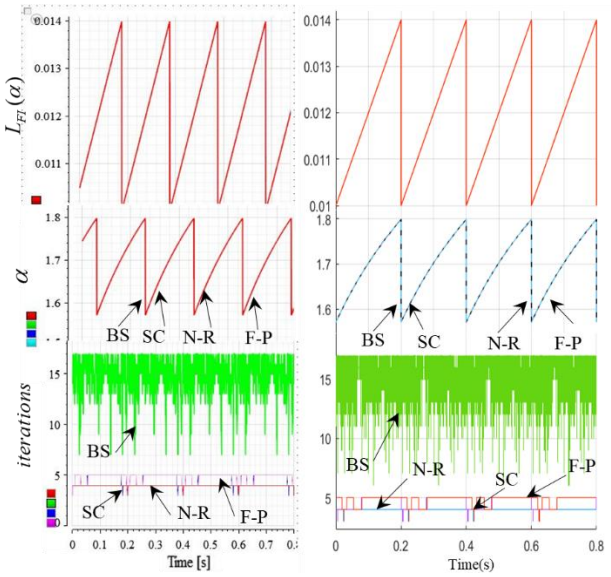

Fig. 15. Real-time verification of the numerical methods in estimating α. (a) signals obtained from the digital signal processor (dSPACE-1006). (b) results obtained in Simulink.

desired variable inductance $L_{FI}(\alpha)$, the firing angle α, and the number of iterations of each numerical method. It is very clear that the results obtained in the real-time digital signal processor accurately match the simulation results in estimating α including the number of iterations of each numerical method. It is noteworthy that these four numerical methods are executed all together concurrently in the dSPACE without causing any overrunning issues, which means that they have an efficient computation burden though the application of only one of them is sufficient to estimate α. Besides, based on both Simulink and real-time applications, it is evident that the N–R has a lower number of iterations (less than 5 iterations) while the BS method has a higher number of iterations (ranges between 17 and 7 iterations).

VI. Conclusion

In this paper, four simple yet-effective numerical algorithms are proposed to extract the firing angle of the FC-TCR compensator. The simulation results are carried out under MATLAB/Simulink environment by modeling the FC-TCR with the electrical power system of a practical hybrid ferry, where it has been proved that FC-TCR compensator based on the proposed methods can effectively reduce the harmonics distortion to meet the IEC 61000-4-7/30 standards and tends the PF towards unity. Moreover, the real-time verification demonstrated that the proposed numerical methods can work effectively when programmed in digital signal processor cards with an efficient computation burden. Based on the conducted analysis, the following remarks are observed:

- Though, the four proposed numerical methods (N–R, BS, FP, SC methods) can provide accurate firing angle estimation, the N–R method seemed to be more effective as it requires a smaller number of iterations.
- Conversely to the traditional methods, The proposed methods can be performed online; hence, they can be adapted under frequency drifts.
- In the studied case, the FC-TCR compensator based on the proposed methods was only applied to a shipboard microgrid. However, it can also be applied to any electrical power system.
- The application of the proposed numerical methods was investigated only for the FC-TCR in this paper. Yet, it is worthy to state that these methods can effectively be applied to controls of different types of SVCs with thyristors.

Appendix

This appendix presents the source code of different numerical methods applied to firing angles estimation for controls of FCTCR used in the study.

A1. The Bisection Method Code in C++ Language Applied to MATLAB Function:

```
function [x1,k2]     = fcn(L,Lpf)  % (L is the TCR
real inductance and Lpf is the variable inductance
obtained by controlling the thyristors of the TCR,
x1 is the estimated firing angle and k2 is the
number of iterations)

y=@(x) (sin(2*x)-2*x+2*pi-((Lpf*pi)/L)); % the non-
linear equation

x1=3; x2=1;  % the initial guesses
k2=0;

if y(x1)*y(x2)>0

    fprintf('no roots exist within the given
interval/n');
    return
end
if y(x1)==0
    fprintf('x1 is one of the roots/n');
    return
elseif y(x2) ==0
    fprintf('x2 is one of the roots/n');
    return
end

 for k=1:100
    xh=(x1+x2)/2;%bisection
    if y(x1)*y(xh)<0;
        x2=xh;
    else
        x1=xh;
    end
    if abs(y(x1))<0.0001;
        break
    end
    k=k+1;
end
k2=k
```

A2. The Newton-Raphson Method Code in C++ Language Applied to MATLAB Function:

```
function [y,k] = fcn(xk,L,Lpf) % (L is the TCR
real inductance and Lpf is the variable inductance
obtained by controlling the thyristors of the TCR,
xk is the initial guess, y is the estimated firing
angle and k is the number of iterations)
```

```
eur=0.0001; % the tolerant error
maxiter=20; % the maximum number of iterations

  o=((Lpf*pi)/L);

for k=1:maxiter
    fx=(sin(2*xk)-2*xk+2*pi-o); % the non-linear
equation

    fpx=(2*cos(2*xk)-2);
    x_imp=xk-(fx/fpx);
    diff=((x_imp-xk)/xk)*100;
    if abs(diff) <= eur  || k>= maxiter
    break
    end
    xk=x_imp;
    k=k+1;
end
y = xk;
```

A3. The False Position Method Code in C++ Language Applied to MATLAB Function:

```
function  [xr,iteration] = FalsePosition(L,Lpf) % (L
is the TCR real inductance and Lpf is the variable
inductance  obtained by controlling the thyristors
of the TCR, xr is the estimated firing angle and
iteration is the number of iterations)

f = @(x) (sin(2*x)-2*x+2*pi-((Lpf*pi)/L)); % the
non-linear equation

iteration=0;
xl=-1;
xu=5;
xr=xl;
error=0.0001;
e=0.0001;
K=0;
if  (f(xl)*f(xu)>0)
    disp('Interval have some error')
else
    fprintf('Itr     XR')
     while ( abs(f(xr)) > e )
         iteration=iteration+1;

        xrOld=xr;
        xr=xu-( (f(xu)*(xl-xu)) /(f(xl)-f(xu)));
        xrNew=xr;
        if f(xl)*f(xr)<0    %
            xu=xr;
        else if f(xl)*f(xr)>0
            xl=xr;

            else
            break
            end
        error=(xrNew-xrOld)/xrNew;
        end
    end
end
end
```

A4. The Scant Method Code in C++ Language Applied to MATLAB Function:

```
function [xn,iter]     = fcn(L,Lpf) % (L is the TCR
real inductance and Lpf is the variable inductance
obtained by controlling the thyristors of the TCR,
xn is the estimated firing angle and iter is the
number of iterations)

iter=0;
maxiter = 20; % maximum number of iteration
f = @(x) (sin(2*x)-2*x+2*pi-((Lpf*pi)/L));
xn_2 = 0.1;
xn_1 = 10;
maxerr = 0.0001;
xn = (xn_2*f(xn_1) - xn_1*f(xn_2))/(f(xn_1) -
f(xn_2));
flag = 1;
while abs(f(xn)) > maxerr
    xn_2 = xn_1;
    xn_1 = xn;
    xn = (xn_2*f(xn_1) - xn_1*f(xn_2))/(f(xn_1) -
f(xn_2));
    iter = iter + 1;
    if(flag == maxiter)
        break;
    end
end
```

REFERENCES

[1] *Control of Harmonics in Electrical Power Systems*, American Bureau of Shipping Guidance, 2006.

[2] S. Jayasinghe, L. Meegahapola, N. Fernando, Z. Jin, and J. Guerrero, “Review of ship microgrids: system architectures, storage technologies and power quality aspects,” *Inventions*, vol. 2, no. 1, p. 4, 2017.

[3] G. Sulligoi, A. Vicenzutti, V. Arcidiacono and Y. Khersonsky, "Voltage stability in large marine-integrated electrical and electronic power systems," *IEEE Trans. on Industry Applications*, vol. 52, no. 4, pp. 3584-3594, Jul.-Aug. 2016.

[4] J. Mindykowski, “Power quality on ships: today and tomorrow’s challenges,” in *Proc. Int. Conf. Expo. Electr. Power Eng.*, pp. 1–18, December 2014.

[5] C. L. Su and C. J. Hong, “Design of passive harmonic filters to enhance power quality and energy efficiency in ship power systems,” in *Proc. 49th IEEE/IAS Industrial & Commercial Power Systems Technical Conference*, pp. 1–8, 2013.

[6] J. Mindykowski, “Case study- based overview of some contemporary challenges to power quality in ship systems,” *Inventions*, vol. 1, no. 4, p. 12, 2016.

[7] Y. Terriche, D. Kerdoun, and H. Djeghloud, “A new passive compensation technique to economically improve the power quality of two identical single-phase feeders,” in *Proc. IEEE 15th Int. Conf. Environ. Electr. Eng. EEEIC 2015 - Conf. Proc.*, no. 2, pp. 54–59, 2015.

[8] Y. Terriche, D. Kerdoun, S. Golestan, A. Laib, H. Djehloud, and J. M. Guerrero, “Effective and low-cost passive compensator system to improve the power quality of two electric generators,” IET Power Electron., vol. 12, no. 7, pp. 1833–1840, Jun. 2019.

[9] An Luo, Zhikang Shuai, Wenji Zhu, Ruixiang Fan, and Chunming Tu, “Development of hybrid active power filter based on the adaptive fuzzy dividing frequency-control method,” *IEEE Trans. Power Deliv.*, vol. 24, no. 1, pp. 424-432, Jan. 2009.

[10] Y. Terriche, S. Golestan, J. M. Guerrero, D. Kerdoune, and J. C. Vasquez, “Matrix pencil method-based reference current generation for shunt active power filters,” *IET Power Electron.*, vol. 11, no. 4, pp. 772–780, Apr. 2018.

[11] A. Hamadi, S. Rahmani, and K. Al-Haddad, “A hybrid passive filter configuration for VAR control and harmonic compensation,” *IEEE Trans. Ind. Electron.*, vol. 57, no. 7, pp. 2419-2434, 2010.

[12] R. M. Mathur and R. K. Varma, *Thyristor-based FACTS Controllers for Electrical Transmission Systems*, John Wiley & Sons, 2002.

[13] L. Wang, C. S. Lam, and M. C. Wong, “Multifunctional hybrid structure of SVC and capacitive grid-connected inverter (SVC//CGCI) for active power injection and nonactive power compensation,” *IEEE Trans. Ind. Electron.*, vol. 66, no. 3, pp. 1660–1670, Mar. 2019.

[14] J. G. Mayordomo, M. Izzeddine and R. Asensi, "Load and voltage balancing in harmonic power flows by means of static VAr compensators," *IEEE Trans. on Power Delivery*, vol. 17, no. 3, pp. 761-769, July 2002.

[15] Y. Terriche, M. U. Mutarraf, M. Mehrzadi, C. Su, J. M. Guerrero and J. C. Vasquez, "More in-depth analytical investigations of two Effective Harmonics Filters for More Electric Marine Vessel Applications," in *Proc. 9th International Conference on Power and Energy Systems* (ICPES), Perth, Australia, 2019, pp. 1-6.

[16] Y. Terriche *et al.*, “A hybrid compensator configuration for VAR Control and harmonic suppression in all-electric shipboard power systems,” *IEEE Trans. Power Deliv.*, vol. 35, no. 3, pp. 1379-1389, June 2020.

[17] L. Lamont and E. Ali Sayigh, *Application of Smart Grid Technologies: Case Studies in Saving Electricity in Different Parts of the World*,

Academic Press, 2018.
[18] I. Abdulrahman and G. Radman, “Wide-area-based adaptive neuro-fuzzy SVC controller for damping interarea oscillations,” *Can. J. Electr. Comput. Eng.*, vol. 41, no. 3, pp. 133–144, Jun. 2018.
[19] L. Wang, C. S. Lam, and M. C. Wong, “Design of a thyristor controlled LC compensator for dynamic reactive power compensation in smart grid,” *IEEE Trans. Smart Grid*, vol. 8, no. 1, pp. 409–417, Jan. 2017.
[20] X. Zhang, B. Li, G. Zhu, X. Chen, and M. Zhou, “Decentralized adaptive quantized excitation control for multi-machine power systems by considering the line-transmission delays,” *IEEE Access*, vol. 6, pp. 61918–61933, 2018.
[21] Y. Mi, C. Ma, Y. Fu, C. Wang, P. Wang, and P. C. Loh, “The SVC additional adaptive voltage controller of isolated wind-diesel power system based on double sliding-mode optimal strategy,” *IEEE Trans. Sustain. Energy*, vol. 9, no. 1, pp. 24–34, Jan. 2018.
[22] Y. Wan, M. A. A. Murad, M. Liu, and F. Milano, “Voltage frequency control using SVC devices coupled with voltage dependent loads,” *IEEE Trans. Power Syst.*, vol. 34, no. 2, pp. 1589–1597, Mar. 2019.
[23] J. Wang, C. Fu, and Y. Zhang, “SVC control system based on instantaneous reactive power theory and fuzzy PID,” *IEEE Trans. Ind. Electron.*, vol. 55, no. 4, pp. 1658–1665, Apr. 2008.
[24] R. A. Mezei, *An Introduction to SAGE Programming*, John Wiley, and Sons, USA, 2016.
[25] Y. Terriche et al., "Harmonics Mitigation in Hybrid AC/DC Shipboard Microgrids Using Fixed Capacitor-Thyristor Controlled Reactors," 2020 IEEE International Conference on Environment and Electrical Engineering and 2020 IEEE Industrial and Commercial Power Systems Europe (EEEIC / I&CPS Europe), Madrid, Spain, 2020, pp. 1-6.
[26] Stoicovici, Dinu IA, Ungureanu, Miorita, Ungureanu, Nicu, et al., "Computer model for sieves' vibrations analysis, using an algorithm based on the false-position method," *American Journal of Applied Sciences*, 2009, vol. 6, no 1, p. 48.
[27] Woodford, Chris, and Chris Phillips, *Numerical Methods with Worked Examples: Matlab Edition*, Springer Science & Business Media, 2011.